InAs/GaAs submonolayer quantum-dot superluminescent diodes with active multimode interferometer configuration*

Li Xin-Kun(李新坤), Jin Peng(金 鹏)†, Liang De-Chun(梁德春), Wu Ju(吴 巨), and Wang Zhan-Guo(王占国)

Key Laboratory of Semiconductor Materials Science and Beijing Key Laboratory of Low-dimensional Semiconductor Materials and Devices, Institute of Semiconductors, Chinese Academy of Sciences, Beijing 100083, *China*

(Received 7 June 2012; revised manuscript received 18 October 2012)

With a chirped InAs/GaAs SML-QD (quantum dot) structure serving as the active region, the superluminescent diodes emitting at wavelength of around 970 nm are fabricated. By using an active multimode interferometer configuration, these devices exhibit high continue-wave output powers from the narrow ridge waveguides. At continue-wave injection current of 800 mA, an output power of 18.5 mW, and the single Gaussian-like emission spectrum centered at 972 nm with a full width at half maximum of 18 nm are obtained.

Keywords: quantum dot, submonolayer, self-assembled, superluminescent diode

PACS: 81.07.Ta, 81.16.Dn, 85.35.Be, 85.60.Jb **DOI:** 10.1088/1674-1056/22/4/048102

1. Introduction

Superluminescent diodes (SLDs) with high output powers and wide emission spectra are attractive for many applications, such as optical fiber sensors,[1] optical coherence tomography (OCT),[2–5] and tunable external cavity lasers.[6–8] In recent years, much research effort has been made to improve the spectral bandwidths and output powers of SLDs. Quantum dots (QDs) with the characteristic of size inhomogeneity, naturally occurring in the epitaxial growth by Stranski–Krastanow (SK) mode, have successfully been used as the active media to broaden the spectral bandwidths of SLDs.[9–14] To achieve high-power operation, different methods have been presented, such as SLDs with the tapered structure[15] and the multi-section device configuration.[16–18] Besides a wide emission spectrum and a high output power, a single transverse mode operation is also required in the practical applications of fiber-optic systems. However, so far, there have been few reports on demonstrating an SLD which has not only a high output power but also single transverse mode.[19]

In this letter, with the chirped InAs/GaAs submonolayer (SML) QDs serving as an active region, the short-wavelength SLDs emitting around 970 nm are fabricated. By using an active multimode interferometer (MMI) configuration, the SLDs exhibit high output powers from the narrow ridge waveguides. It is demonstrated that the QD-SLDs with the active MMI configurations can improve heat dissipation and optical performance compared with the SLDs with the regular tilted-waveguide structure.

2. Experiments

The epitaxial structures for the SML-QD SLD devices in this study are grown by a Riber 32P solid-source molecular beam epitaxy (MBE) machine on n-GaAs (001) substrates as reported in our previous study.[20] The active region of the devices consists of a chirped InAs/GaAs SML-QD structure, which comprises 12 InAs/GaAs SML-QD layers to broaden the emission spectra from the SML-QD SLDs. In the chirped SML-QD structure, each QD layer is formed by ten-cycled deposition of InAs and GaAs. In the ten epitaxial deposition cycles, the deposition amounts of GaAs are all 2.25 ML, while the deposition amounts of InAs are 0.25 ML, 0.25 ML, 0.30 ML, 0.30 ML, 0.35 ML, 0.35 ML, 0.40 ML, 0.40 ML, 0.40 ML, 0.45 ML, 0.45 ML, and 0.45 ML, respectively. The whole active region is sandwiched between 1.5-μm n- and p-type $Al_{0.5}Ga_{0.5}As$ cladding layers. Finally, a p^+-doped GaAs contact layer completes the epitaxial structure.

With the chirped InAs/GaAs SML-QD structure serving as an active region, the QD-SLD devices, each with a ridge waveguide, are fabricated by using the standard photolithography process and inductively coupled plasma (ICP) etching. The 1×1 multimode interferometer is designed and fabricated for the active MMI QD-SLD device (SLD-1) as shown in Fig. 1(a). The width of the single-mode waveguide is 5 μm, while the width of the multi-mode waveguide is 10 μm. To relax fabrication tolerance for the multimode interferometer, a 20-μm-length tapered region is used at both the beginning and the end of the multi-mode waveguide.[21] For comparison, we also fabricate a tilted-waveguide SLD (SLD-2) with 5-μm-

*Project supported by the National Basic Research Program of China (Grant No. 2006CB604904) and the National Natural Science Foundation of China (Grant Nos. 60976057, 61274072, and 60876086).

†Corresponding author. E-mail: pengjin@semi.ac.cn

© 2013 Chinese Physical Society and IOP Publishing Ltd

wide ridge on the same wafer as shown in Fig. 1(b). The actually implemented waveguide of the QD-SLD device is tilted with an angle of 6° with respect to the facet normal, with $\lambda/4$ SiO_2 AR coatings on both facets of the devices to suppress facets? reflectivity. All the devices are mounted p-side down on the copper heatsinks and tested at room temperature (RT).

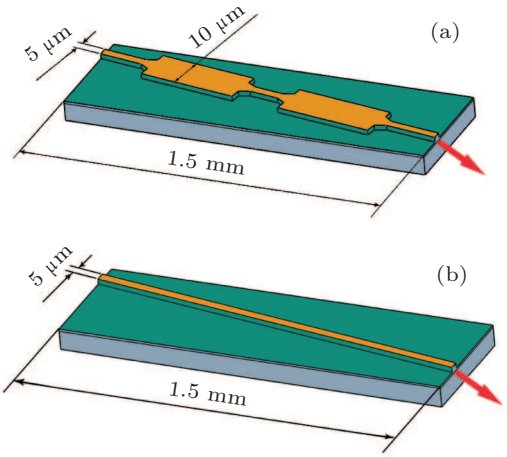


Fig. 1. (color online) Schematics of active MMI SLD (a) and tilted-waveguide SLD (b).

3. Results and discussion

Figures 2(a) and 2(b) exhibit the voltage–current (*I*–*V*) and power–current (*P*–*I*) characteristics of the QD-SLD devices under continue-wave (CW) operation, respectively. From the *I*–*V* curve as shown in Fig. 2(a), it can be observed that the driving voltage of device SLD-1 is lower than that of device SLD-2. This is mainly due to the low differential resistance by using MMI configuration, compared with that of tilted-waveguide SLD. The obtained differential resistances are 0.35 Ω and 0.73 Ω for the active MMI SLD and the tilted-waveguide SLD, respectively. In comparison, the device SLD-1 with an active MMI configuration is obviously superior in wall-plug power consumption. For instance, at the same output power of 7 mW, the power consumption is 0.95 W for the active MMI QD-SLD, while it is 1.1 W for the tilted-waveguide QD-SLD. From the *P*–*I* curve in Fig. 2(b), two almost identical turn-on currents are obtained for both types of QD-SLDs. This implies that there is no significant excess-loss in the SLD device with the active MMI configuration. At a CW injection current of 800 mA, an output power of 18.5 mW is obtained from the active MMI QD-SLD, which increases 10 mW, i.e., 1.2 times larger than that of the tilted-waveguide QD-SLD. By using the active MMI configuration, high output power is achieved, owing to the wider actively pumped area, which contributes to improving the power saturation level.

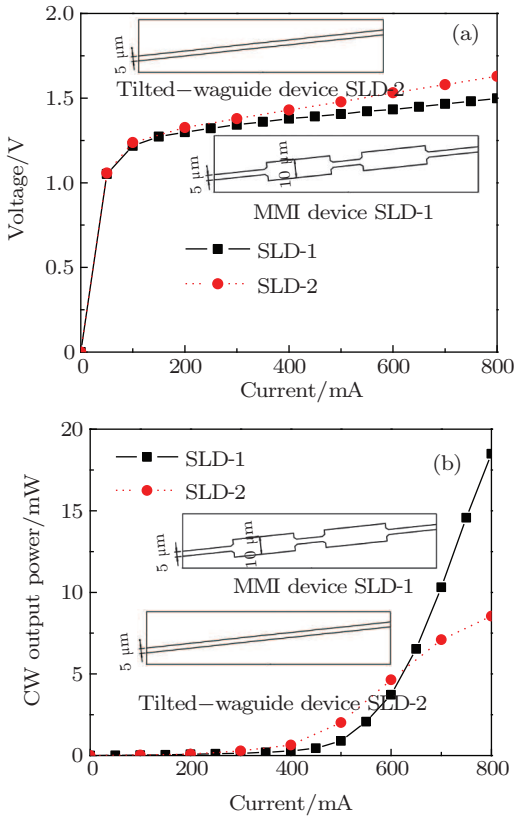


Fig. 2. (color online) *I*–*V* (a) and *P*–*I* (b) characteristics of the QD-SLD devices. The devices SLD-1 and SLD-2 are with active MMI structure and tilted-waveguide structure, respectively.

Figures 3(a) and 3(b) show the pulsed (pulse width: 30 μs, repetition rate: 1 kHz) and CW *P*–*I* characteristics, respectively, for both device SLD-1 and SLD-2. As shown in the figure, under pulsed operation, the typical superluminescent characteristics are observed from the *P*–*I* curves of both types of QD-SLDs. At a pulsed injection current of 800 mA, two almost identical output powers (∼ 25 mW) are obtained from both types of QD-SLDs. However, under CW operation, an output power is achieved to be as high as 18.5 mW from the QD-SLD with the active MMI configuration, while, only an output power of 8.5 mW is obtained as a result of the significant power saturation from the tilted-waveguide QD-SLD. Therefore, it is concluded that the output power saturation is caused mainly by self-heating in the active region of an SLD device. In the QD-SLD with the active MMI configuration, the thermal roll-over of output power is significantly improved, which mainly benefits from the reduced thermal resistance. With the increase of the active area size, the heat source dissipates much more effectively as a result of a broader heat spreading path to the heatsink. Another reason is that the wide active area reduces the series resistance which is primarily responsible for the self-heating in the active region.

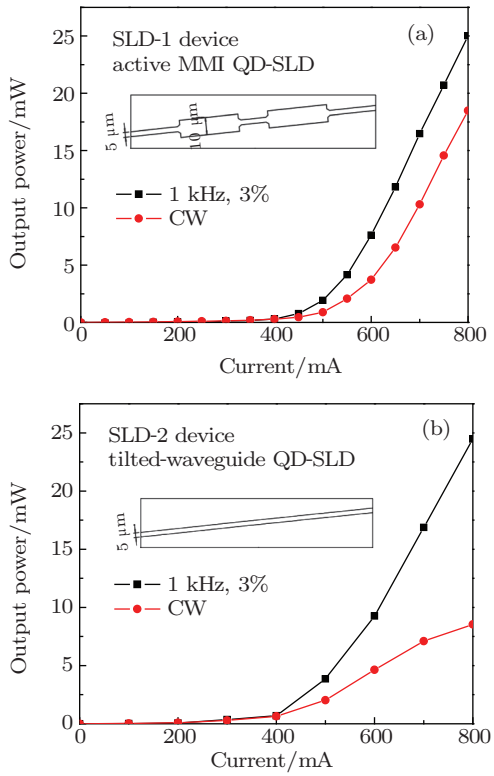


Fig. 3. (color online) Pulsed and CW *P–I* characteristics for the devices SLD-1 (a) and SLD-2 (b), respectively.

Figure 4 shows the electroluminescence (EL) spectra of the active MMI QD-SLD at different injection currents under CW operation. At a low injection current of 20 mA, an emission spectrum centered at 996 nm with an FWHM of 62 nm is obtained. At the low injection level, the wide spectrum is dominated by the overlapping of spontaneous emissions from different SML-QD layers of the chirped InAs/GaAs SML-QD active region. With injection current increasing from 20 mA to 800 mA, the emission spectrum from the device becomes narrow gradually due to the increasing of stimulated radiation at the high injection level. Owing to the exponential relation between the output power spectrum and the gain spectrum resulting from stimulated radiation, the spectral bandwidth of the devices is reduced. A spectral blue-shift in the emission spectrum of the SLD device is also observed with the increase of injection current. It is attributed to the carrier transfer to the SML-QD layers with larger InAs deposited amounts under lower injection level, and also to the increase of carrier filling in the SML-QD layers with lower InAs deposited amounts, corresponding to the shorter wavelength emission, under higher injection. As shown in Fig. 4, a blue-shift of the EL peak from 996 nm to 972 nm is observed with injection current increasing from 20 mA to 800 mA. At a CW injection current of 800 mA, an emission spectrum centered at 972 nm with a full width at half maximum (FWHM) of 18 nm is obtained. The SLD having a Gaussian-like spectrum with a single peak is applicable to the ophthalmology OCT. It is also observed from the figure that a spectral modulation appears in the emission spectrum at an injection current of 800 mA, which may be due to internal reflection and scattering caused by the large sidewall roughness of MMI waveguide occurring in the ICP etching process. It is expected that higher performance can be obtained with an optimized etching process during the fabrication of the devices.

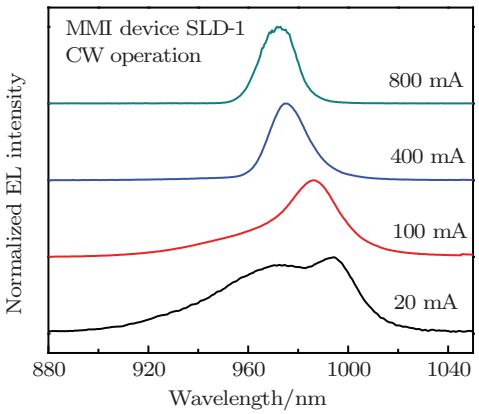


Fig. 4. (color online) EL spectra of the active MMI QD-SLD at different injection currents under CW operation.

4. Conclusion

In the present paper, we present a short-wavelength emitting at around 970 nm from the QD-SLD with the chirped InAs/GaAs SML-QD serving as an active region. By using the active MMI configuration, the QD-SLD exhibits relatively high output power from a narrow ridge waveguide of 5 μm in width, which can be coupled into regular single-mode fibers without using additional output mode trimming devices. Furthermore, it is demonstrated that a reduced thermal resistance and improved performance can be achieved in the high-power SLD with the active MMI configuration. At a CW injection current of 800 mA, an output power of 18.5 mW and an emission spectrum centered at 972 nm with an FWHM of 18 nm are obtained. Such an SLD with the wavelength less than 1 μm and a single Gaussian-like spectral shape is very attractive due to the need of miniaturized, low cost and high-resolution OCT systems for ophthalmology OCT imaging.

References

[1] Lee B 2003 *Opt. Fiber Technol.* **9** 57
[2] Schmitt J M 1999 *IEEE J. Sel. Topics Quantum Electron.* **5** 1205
[3] Zotter S, Pircher M, Torzicky T, Bonesi M, Götzinger E, Leitgeb R A and Hitzenberger C K 2011 *Opt. Express* **19** 1217
[4] Wang K, Zeng Y, Ding Z H, Meng J, Shi G H and Zhang Y D 2010 *Acta Phys. Sin.* **59** 2471 (in Chinese)
[5] Liang Y M, Zhou D C, Meng F Y and Wang M W 2007 *Acta Phys. Sin.* **56** 3246 (in Chinese)
[6] Lü X Q, Jin P, Wang W Y and Wang Z G 2010 *Opt. Express* **18** 8916

[7] Lü X Q, Jin P and Wang Z G 2010 *Chin. Phys. B* **19** 018104
[8] Wu J, Lü X Q, Jin P, Meng X Q and Wang Z G 2011 *Chin. Phys. B* **20** 064202
[9] Rossetti M, Li L H, Markus A, Fiore A, Occhi L, Vélez C, Mikhrin S, Krestnikov I and Kovsh A 2007 *IEEE J. Quantum Electron.* **43** 676
[10] Lü X Q, Liu N, Jin P and Wang Z G 2008 *IEEE Photon. Technol. Lett.* **20** 1742
[11] Zhang Z Y, Jiang Q, Hopkinson M and Hogg R A 2010 *Opt. Express* **18** 7055
[12] Zhang Z Y, Hogg R A, Lü X Q and Wang Z G 2010 *Adv. Opt. Photon.* **2** 201
[13] Jiang Q, Zhang Z Y, Hopkinson M and Hogg R A 2010 *Electron. Lett.* **46** 295
[14] Liang D C, An Q, Jin P, Li X K, Wei H, Wu J and Wang Z G 2011 *Chin. Phys. B* **20** 108503
[15] Haffouz S, Barrios P J, Normandin R, Poitras D and Lu Z 2012 *Opt. Lett.* **37** 1103
[16] Du G T, Devane G, Stair K A, Wu S L, Chang R P H, Zhao Y S, Sun Z Z, Liu Y, Jiang X Y and Han W H 1998 *IEEE Photon. Technol. Lett.* **10** 57
[17] Greenwood P D L, Childs D T D, Groom K M, Stevens B J, Hopkinson M and Hogg R A 2009 *IEEE J. Sel. Top. Quantum Electron.* **15** 757
[18] Li X K, Jin P, An Q, Wang Z C, Lü X Q, Wei H, Wu J, Wu J and Wang Z G 2012 *Opt. Express* **20** 936
[19] Zang Z G, Minato T, Navaretti P, Hinokuma Y, Duelk M, Velez C and Hamamoto K 2010 *IEEE Photon. Technol. Lett.* **20** 721
[20] Li X K, Liang D C, Jin P, An Q, Wei H, Wu J and Wang Z G 2012 *Chin. Phys. B* **21** 028102
[21] Zhang M, Krüger A C, Groothoff N, Balle T and Kristensen M 2011 *Opt. Lett.* **36** 3058